

This is an Open Access document downloaded from ORCA, Cardiff University's institutional repository: <https://orca.cardiff.ac.uk/id/eprint/146390/>

This is the author's version of a work that was submitted to / accepted for publication.

Citation for final published version:

Chen, Jing , Han, Qian, Ryu, Doojin and Tang, Jing 2022. Does the world smile together? A network analysis of global index option implied volatilities. *Journal of International Financial Markets, Institutions and Money* 77 , 101497. 10.1016/j.intfin.2021.101497

Publishers page: <https://doi.org/10.1016/j.intfin.2021.101497>

Please note:

Changes made as a result of publishing processes such as copy-editing, formatting and page numbers may not be reflected in this version. For the definitive version of this publication, please refer to the published source. You are advised to consult the publisher's version if you wish to cite this paper.

This version is being made available in accordance with publisher policies. See <http://orca.cf.ac.uk/policies.html> for usage policies. Copyright and moral rights for publications made available in ORCA are retained by the copyright holders.



Does the world smile together? A network analysis of global index option implied volatilities

Jing Chen^a, Qian Han^{b,*}, Doojin Ryu^{c,*}, Jing Tang^d

^a *School of Mathematics, Cardiff University, Cardiff, United Kingdom*

^b *Wang Yanan Institute for Studies in Economics, Xiamen University, Xiamen, Fujian, China*

^c *Department of Economics, Sungkyunkwan University, Seoul, Korea*

^d *Zheshang Securities Co. Ltd., Hangzhou, China*

* Corresponding authors (sharpjin@skku.edu)

E-mail addresses: chenj60@cardiff.ac.uk (J. Chen), hanqian@xmu.edu.cn (Q. Han), sharpjin@skku.edu (D. Ryu), tangjing93@foxmail.com (J. Tang).

Acknowledgments

We extend our gratitude to Jonathan Batten (the Editor) and Jinyoung Yu. Qian Han is supported by the National Science Foundation of China (No. 71631004).

Highlights

- We provide strong evidence of contagion among global index options markets.
- A directed acyclic graph analysis reveals strong regional implied volatility clustering.
- No options market is completely independent of the others in the long run.
- Implied volatility spillovers are more intense when markets experience crises.

Abstract

This study uses directed acyclic graph and spillover index models to find significant evidence of both implied volatility contagion and spillovers. First, we observe strong regional clustering among the implied volatility smiles of global markets. European and American options markets form a separate contemporaneous contagion cluster from markets in the Asia-Pacific region. However, no market is completely independent from the markets in the other two regions in the long run. The European index options markets demonstrate the strongest implied volatility smile contagion.

Second, we observe the heterogeneity across different markets in terms of implied volatility spillover, and extreme market conditions, such as crises, seem to intensify the spillover effects. The trend in the short-run underlying index return, the implied volatility of at-the-money options, and the interest rate term spread are key determinants of implied volatility spillovers.

Keywords: Contagion; Directed acyclic graph; Global index options markets; Implied volatility smile; Volatility spillover

JEL Classification: G11, G13, G15

1. Introduction

The Black–Scholes model suggests that, in theory, the implied volatility is not connected to the exercise price of a specific option. However, in real-world financial markets, the implied volatility increases as options contracts become increasingly in or out of the money. As a result, the option implied volatility smile is one of the best-known financial anomalies. Some scholars believe that this puzzle is due to the unrealistic assumptions made in the Black–Scholes model (e.g., Eraker, Johannes, and Polson, 2003; Hull and White, 1987; Kim and Ryu, 2015; Ryu, Kang, and Suh, 2015). Others suggest that the observed volatility smile arises because of market behavior. For example, Pena, Rubio, and Serna (1999) find that implied volatility smiles are positively correlated with trading costs and volumes and negatively correlated with historical volatilities and expiry dates. Many other factors can explain the shape of the volatility smile as well, including net buying pressure (Bollen and Whaley, 2004; Ryu, Ryu, and Yang, 2021; Ryu, Webb, Yang, and Yu, 2022; Ryu and Yang, 2022), investor sentiment (Han, 2008), systemic risk factors (Duan and Wei, 2009), the liquidity of options and spot markets (Chou, Chung, Hsiao, and Wang, 2011), and heterogeneity in investors’ beliefs (Friesen, Zhang, and Zorn, 2012).¹

¹ Some studies examine the differing responses of the prices of options with different moneyness levels to the same underlying price changes (Bakshi, Cao, and Chen, 2000; Sim, Ryu, and Yang, 2015; Yang, Choi, and Ryu, 2017). These studies highlight violations of option price monotonicity. Considering that levels of and changes in implied volatilities are determined by the price dynamics of the underlying assets and options contracts, the topic is also related to our study.

Nevertheless, we should not forget that, because options are traded globally, implied volatilities have both time-varying and cross-sectional features, such as lead-lag effects across different countries and regions. Contemporary investors can access more markets through advancements in financial technologies, and they must fully understand complex aspects of trading, such as buying pressure. Studying implied volatilities and their interdependence, as opposed to time-varying volatility spillovers, can help achieve understanding practical aspects of investing. This understanding can enable portfolio optimization and risk management from a forward-looking perspective.

Unfortunately, research on this topic is limited. To fill this gap, we conduct a cross-market study of both implied volatility smile contagion and spillover effects across global index options markets. Our data cover 25 countries and regions worldwide over the period from January 1, 2006, to November 9, 2017. First, we address the cross-sectional contagion effects of implied volatilities by analyzing the features of volatility smiles. We examine, first, whether volatility smiles can explain contagion. Second, we investigate the complex structure through which contemporaneous or lagged contagion spreads in a large global network. It is important to understand which markets strongly dominate others and drive the lead-lag effects.

We examine the time-varying and total volatility spillovers at the aggregate level in each market and across the entire global network under both normal and crisis conditions. In particular, when we include all the index options markets in one complex network, we can better understand the dynamics of the information flows within individual markets, between markets, and across the entire network. To further understand the more complex information transmission process and the increased intensity of contagion, we apply the directed acyclic graph (DAG) method (Awokuse, 2006; Pearl, 1995; Spirtes, Glymour, and Scheines, 2000) to this classic finance problem.

To the best of our knowledge, this study is the first network analysis of global index options markets. Importantly, this method effectively mitigates many drawbacks of the classic methods. Granger causality tests are sensitive to the optimal lags chosen, as the lags affect the robustness of the test results; thus, these tests have limitations in studying the causal relationships among multiple variables, as in the context of this study. The impulse response and variance decomposition analysis

methods allow for multivariate analyses of contagion effects by decomposing information shocks. However, these methods require appropriate variable ordering with support from either theory or heuristic prior judgments. For example, classic orthogonal decomposition methods, such as the Cholesky decomposition method, rely heavily on subjective priors rather than on solid theoretical foundations (Swanson and Granger, 1997; Yang and Zhou, 2013). In contrast, the DAG model does not face any of these limitations. It offers a flexible modeling framework for estimating causal relationships in a complex system. For example, our model is based on 25 markets. Using traditional methods to obtain the variance/covariance matrix for a 25×25 vector autoregression (VAR) requires incredibly complicated and dense computations. Certain issues, such as variable ranking and decomposition, may be more pressing in this context. However, the DAG method utilizes high computational algorithms to obtain clusters and causal relations in a large, high-dimensional network. In addition, the DAG provides direct visualization of the contagion clusters among the global index options markets. The directed flows indicate clear causal relationships and reveal price discoveries between the markets.

Our tests start by obtaining the slope of each index options market's volatility smile to establish a VAR model that identifies the lead-lag relations. Next, we extract VAR residuals and construct a DAG to examine the contemporaneous contagion effects among the implied volatilities of the global options markets that we study. These contagion effects directly reflect the causal relationships among these markets and enable us to build a structural VAR (SVAR) model. With this model, we can further study the contemporaneous, short-term, and medium-to-long-term contagion effects for spillovers across the whole network and time-varying spillovers in individual markets. Again, this method avoids the variable ranking issues that commonly appear in the Cholesky variance decomposition. Finally, we investigate the possible economic determinants of network contagion.

One important finding of this study is that the levels, slopes, and curvatures of volatility smiles have direct implications for trading. The level of a volatility smile approximates the overall riskiness of the market, but the levels of actual volatility smiles tend to remain stable over time. Thus, these levels may not be useful for meaningful forecasting. Our pilot test using the implied volatility smiles

of the United States (U.S.), Germany, Japan, and India (Figure 1) clearly illustrates this result.²

[Insert Figure 1 Here]

In contrast, the movements of the slopes are dramatic and, thus, the slope may contain richer information than the levels do. Theoretically, the slope of an implied volatility smile indicates the market hedging pressure. In a real-world financial market with limited arbitrage, the options supply curve should be upward-sloping rather than horizontal. Thus, the net demand for options is positively related to their prices. When investors worry about a potential decline in the spot market, the demand for deep out-of-the-money put options increases sharply, thereby increasing option prices. As a result, the slope of the left side of the implied volatility smile steepens. This idea is supported both theoretically and empirically by Bollen and Whaley (2004), Chan, Cheng, and Lung (2004), and Garleanu, Pedersen, and Poteshman (2009). In addition, Han, Liang, and Wu (2016) explain that the slope of the right side of an implied volatility smile indicates investors' speculative demand. Investors tend to purchase out-of-the-money call options if they speculate that the market may rise in the future.

Moreover, the slope of an implied volatility smile may indicate future market conditions. When a market reaches a low point or volatility is high, the implied volatility in that market generally becomes flatter when the probability of a market rebound is higher. This information is valuable to investors. For instance, the Chicago Board Options Exchange's SMILE Index is based on the slopes of implied volatility smiles, and investors have used it as a primary indicator of the options market since 1986.³

Overall, our results suggest that implied volatilities tend to smile together, but they spread across countries and regions with strong geographic features. For example, Europe and America are connected in the same contagion cluster and are separate from the Asia-Pacific region. In addition,

² We standardize the data when we plot volatility smiles.

³ We also model the levels and curvatures of the volatility smiles using the VAR and DAG approaches and obtain qualitatively similar results. For brevity, we do not report the results here, but they are available upon request.

certain individual markets, such as the U.S. market, have clear spillover effects on other markets. When we study 30-day lags, we find that these markets are well-connected and interdependent. We also find that extreme market conditions, such as the recent financial crisis, amplify contagion effects. Finally, the short-run trend in the underlying index, the historical volatility, the volatility implied by at-the-money (ATM) options, and the interest rate term spread are among the determinants that influence the dynamics of implied volatility smile contagion.

The remainder of this paper is organized as follows. Section 2 reviews the literature. Section 3 introduces the modeling framework, including the SVAR, DAG, and spillover models, and the methodology. Section 4 describes the data, including descriptive statistics and data processing to address asynchronization issues across the global options markets. Sections 5 and 6 report the empirical results of the DAG approach and the spillover models, respectively, and discuss the dynamic features and determinants of spillover effects. Section 7 concludes.

2. Literature Review

2.1. Contagion in Financial Markets

The literature on contagion can be traced back to many studies conducted after the 1987 financial crisis (e.g., Hamao, Masulis, and Ng, 1990; Koutmos and Booth, 1995; Worthington and Higgs, 2004) and the 2008 global financial crisis (e.g., [Baruník, Kočenda, & Vácha, 2016](#); Daly, Batten, Mishra, and Choudhury, 2019; Kim, Ryu, and Seo, 2015; Sewraj, Gebka, and Anderson, 2018). Studies of cross-asset contagion are also carried out. The majority suggests that correlations among the same assets, such as stocks, across markets, generally increase over time, whereas correlations between different assets across markets tend to decrease (e.g., Gulko, 2002; Kim, Moshirian, and Wu, 2006). However, Forbes and Rigobon (2002) suggest that these estimated correlations between cross-market stock returns tend to be biased and that the spillover effects mostly disappear when these biases are corrected. Briere, Chapelle, and Szafarz (2012) reject the spillover hypothesis for fixed income assets, although they accept that spillovers among stocks exist as a result of financial globalization. Chan-Lau, Mathieso, and Yao (2004) suggest that the magnitudes and scales of spillovers are often linked to the initiating country's economic

fundamentals and risk exposure. In contrast, Connolly and Wang (2003) propose that spillovers of private rather than public information may be the main driver of the co-movements of stock prices in international markets. In addition to these studies, some similar efforts have been made in the literature on the options markets as well (Finta and Aboura, 2020; Gemmill and Kamiyama, 2000; Greenwood-Nimmo, Nguyen, and Rafferty, 2016; Lin, Engle, and Ito, 1994; Narwal, Sheera, and Mittal, 2012; Shu and Chang, 2019).

2.2. Methods of Measuring Financial Contagion

Although financial contagion is inevitably important and influential, no universally accepted definition of contagion exists because of the complexity of the information shock transmission process (e.g., Chang and Majnoni, 2002; Corsetti, Pericoli, and Sbracia, 2005). Masson (1999) suggests that only a model with multiple equilibria that can handle the transmission of information from both fundamentals and exogenous shocks can detect true contagion. However, other studies, including that of Morris and Shin (2000), have reservations on the multi-equilibria argument as it narrowly equates contagion to spillover effects (Bessler and Yang, 2003; Yang and Bessler, 2004). Moreover, Boyer, Kumagai, and Yuan (2006) argue that methods to detect contagion must exclude the impacts of common shocks (i.e., fundamentals).

Regarding the modeling of contagion, early studies try to directly estimate the correlation coefficients or conditional covariances among financial variables. However, Forbes and Rigobon (2002) argue that high correlations may not necessarily indicate contagion but rather may be the outcomes of changes in the relevant countries' economic fundamentals, risk perceptions, and preferences. For example, if two markets are highly correlated, dramatic changes in one market naturally lead to similar changes in the other. Thus, only a significant increase in the correlation between the two can be considered proof of contagion.

The common method of contagion analysis is to typically conduct a variance decomposition and an impulse response analysis, normally with a VAR model (Eun and Shim, 1989). Diebold and Yilmaz (2009) propose measuring the degree of financial contagion with a volatility spillover index. Diebold and Yilmaz (2012) use the generalized variance decomposition method to enhance the

robustness of their estimations. Both studies suggest that the overall spillover index reflects aggregate contagion. The greater this index is, the more likely it is that market fluctuations are driven by contagion. This method has the clear advantage of quantifying the degree to which each market responds to information shocks from other markets, thereby establishing a ranking of contagion response markets. We, therefore, adopt this method for analyzing the implied volatility smile contagion among global index options markets.

3. Methodologies

Our goal is to examine the contagion effects among 25 individual index options markets worldwide. We focus on implied volatility smiles, especially their slopes, because they provide the practical benefit of indicating real market conditions, such as hedging pressure and future market movements. First, we measure the cross-sectional contagion in this global network so that we can observe the interactions among different markets on the whole. We identify contagion and clusters and the markets that dominate others. After creating a holistic picture of the global index options market, we explore the time-varying contagion across markets.

To fulfill the above, we construct basic VARs for the slopes of the individual markets' implied volatility smiles. We then obtain the residuals from these VARs and use them as inputs to establish our global index options DAG network. The DAG explains the overall causal relationships between individual index options markets. These relationships indicate the cross-sectional contagion effects among the index options markets. We further establish an SVAR model using the causal parameters of the DAG. Unlike the Cholesky decomposition, this model is not heavily dependent on the variable ranking. This allows us to further expand Diebold and Yilmaz's (2009, 2012) spillover index model to thoroughly understand the time-varying volatility within the global network. We can compare contemporaneous, short-term, and medium-to-long-term (lagged) contagion effects and analyze total and directed spillover effects. We describe the technical details of our empirical process in the following subsections.

3.1. DAG Model

Following Bessler and Loper (2001) and Bessler and Yang (2003), we may consider a set of variables $\{V, W\}$ in which each variable represents a node in a graph and the nodes can be connected by edges. Consequently, they form different types of graphs: (1) an undirected graph that has undirected edges (e.g., $V-W$); (2) a directed graph that has unidirectional edges (e.g., $W \rightarrow V$); (3) an oriented graph that has both unidirectional and bidirectional (e.g., $V \leftrightarrow W$) edges; and (4) finally a mixed graph that has unidirectional, bidirectional, and undirected edges.

A DAG can visually show whether the causal flows of a set of variables contain cyclic relationships. The directed edges in a DAG are established by calculating the conditional correlations between the variables or establishing their independence. A DAG presents a non-time sequence that is often a full circle of directed causal flows among variables. Thus, this method is more flexible than the commonly used Granger causality test, especially in the presence of asymmetric information flows (Yang and Zhou, 2013).

We can use the following algorithm to generate a DAG (Bessler and Yang, 2003):

$$\Pr(v_1, v_2, v_3, \dots, v_n) = \prod_{i=0}^n \Pr(x_i | pa_i), \quad (1)$$

where P_r is the probability of nodes $(v_1, v_2, v_3, \dots, v_n)$ and pa_i is the history of the subsets of these variables prior to the realization of v_i . Pearl (1995) calls this concept “d-separation,” and Spirtes, Glymour, and Scheines (2000) develop an algorithm, known as the PC algorithm,⁴ to determine the directions of the causal relationships among variables using a stepwise procedure that reduces the number of edges and orients the directions of the edges between the variables.

⁴ The PC algorithm is programmed in Tetrad III software (<https://www.phil.cmu.edu/projects/tetrad/old/tet3/master.htm>). The specifics of this algorithm are provided in the appendix.

3.2. Spillover Index Model

Consider a VAR model with n variables and p lags:

$$x_t = \phi_1 x_{t-1} + \phi_2 x_{t-2} + \dots + \phi_p x_{t-p} + \varepsilon_t, \quad (2)$$

where $x_t = (x_{1,t}, x_{2,t}, \dots, x_{n,t})'$ is a set of endogenous variables, $\phi_i (i = 1, 2, \dots, p)$ is an $n \times n$ matrix of the parameters, and ε_t are residuals that are independent and identically distributed with $\varepsilon_t \sim N(0, \Sigma)$. Assuming that the covariance matrix is stationary, the VAR model can be rewritten as follows:

$$x_t = \sum_{i=0}^{\infty} A_i \varepsilon_{t-i}, \quad (3)$$

where A_i is an $n \times n$ parameter matrix such that $A_i = \phi_1 A_1 + \phi_2 A_2 + \dots + \phi_p A_{i-p}$ ($i > 0$) and $A_i = 0$ ($i < 0$). A_0 is the identity matrix.

In the variance decomposition process, we use H-step forecasting for the variables x_i ($i = 1, 2, \dots, p$) driven by endogenous shocks, and we collect the proportion of the forecasted errors in the variance resulting from exogenous shocks. We follow Koop, Pesaran, and Potter (1996), Pesaran and Shin (1998), and Diebold and Yilmaz (2012) in using a decomposition process that compensates for the Cholesky decomposition's heavy dependence on the variable ranking. In particular, these are based on a generalized VAR that separately examines the impacts of individual variables; the impacts of the shocks are aggregated at the end of the process, instead of using the static shock impact in the Cholesky decomposition or an SVAR model.

The H-step forecasting error variance decomposition matrix can be defined as:

$$\theta_{ij}^g(H) = \frac{\sigma_{ii}^{-1} \sum_{h=0}^{H-1} (e_i' A_h \Sigma e_j)^2}{\sum_{h=0}^{H-1} (e_i' A_h \Sigma A_h' e_j)}, \quad (4)$$

where $H = 1, 2, \dots, \Sigma$ is the covariance matrix of ε_t , σ_{ii} is the standard deviation of the i th error

term, and e_i is the row vector in which the i th element equals one and the other elements equal zero. When $i = j$, we obtain the variance that records all the endogenous shocks, and when $i \neq j$, we obtain the correlation between the generalized forecast orthogonalized error variances, which indicates the proportion of the shocks in i that are exogenously caused by j .

In a generalized VAR model, the information shocks to each variable are not orthogonal. Thus, the sum of the estimated errors in the variance may not necessarily sum to one. That is, $\sum_{j=1}^n \theta_{ij}^g(H) \neq 1$. To standardize this value, we let

$$\bar{\theta}_{ij}^g(H) = \frac{\theta_{ij}^g(H)}{\sum_{j=1}^n \theta_{ij}^g(H)} \text{ such that } \sum_{j=1}^n \bar{\theta}_{ij}^g(H) = 1 \text{ and } \sum_{i,j=1}^n \bar{\theta}_{ij}^g(H) = n. \quad (5)$$

The total spillover index shows the aggregated contribution of the spillovers among all the variables to the total forecasted error in the variances. This index can be calculated as:

$$S^g(H) = \frac{\sum_{i,j=1, i \neq j}^n \bar{\theta}_{ij}^g(H)}{\sum_{i,j=1}^n \bar{\theta}_{ij}^g(H)} \times 100 = \frac{\sum_{i,j=1, i \neq j}^n \bar{\theta}_{ij}^g(H)}{N} \times 100. \quad (6)$$

The directed spillovers can be determined to help identify the directions of the spillovers. $S_i^g(H)$ is the outflow spillover, and $S_L^g(H)$ is the inflow spillover, indicating the spillovers of a variable to and from other variables, respectively:

$$S_i^g(H) = \frac{\sum_{j=1, i \neq j}^n \bar{\theta}_{ji}^g(H)}{\sum_{j=1}^n \bar{\theta}_{ij}^g(H)} \times 100 \text{ and } S_L^g(H) = \frac{\sum_{j=1, i \neq j}^n \bar{\theta}_{ij}^g(H)}{\sum_{j=1}^n \bar{\theta}_{ij}^g(H)} \times 100. \quad (7)$$

The net spillover index $s_i^g(H)$ is the difference between the outflow and inflow spillovers:

$$S_i^g(H) = S_i^g(H) - S_L^g(H). \quad (8)$$

Further, the net cross-spillover between variables, $S_{ij}^g(H)$, can be calculated as follows:

$$S_{ij}^g(H) = \left(\frac{\bar{\theta}_{ji}^g(H)}{\sum_{i=1}^n \sum_{k=1}^n \bar{\theta}_{ik}^g(H)} - \frac{\bar{\theta}_{ij}^g(H)}{\sum_{j=1}^n \sum_{k=1}^n \bar{\theta}_{jk}^g(H)} \right). \quad (9)$$

Equivalently, it can be written as follows:

$$S_{ij}^g(H) = \left(\frac{\bar{\theta}_{ji}^g(H) - \bar{\theta}_{ij}^g(H)}{n} \right). \quad (10)$$

4. Data

4.1. Descriptive Statistics

Globally, 26 markets across Asia, Australia, Europe, and the Americas offer stock index options. We include 25 of them in our sample, excluding Singapore's options market because it uses other countries' and regions' indices as its options' underlying assets. Options contracts approaching their maturity dates tend to be more liquid. Hence, we use data on near-month contracts with moneyness levels of 90%, 95%, 100%, and 105% taken from Bloomberg terminals to study their implied volatilities⁵ for the period from January 3, 2005, to November 9, 2017. Table 1 lists the names, years in existence, and associated exchanges of each index option, and Table 2 reports descriptive statistics for the data. The mean values of the implied volatilities of Greece, Russia, and Italy are among the highest, whereas the corresponding means for Denmark, the U.S., and Israel are the lowest. In terms of standard deviations, Italy, Canada, and Norway are the most volatile, whereas Brazil, Denmark, and Israel are the least volatile.

[Insert Table 1 Here]

[Insert Table 2 Here]

⁵ If a country or region has more than one index option, we use the index option with the highest daily trading volume.

4.2. Asynchronization of Trading Times across Markets

The trading times of these exchanges span four continents, thus, are not synchronized. Some markets (e.g., Japan, Taiwan, and the U.S.) have electronic trading platforms that cover hours outside of normal trading times. To ensure synchronization, we map the trading times of the 25 markets to Beijing time (see Figure 2). Furthermore, in a global network, the trading times in different geographic markets may overlap. The overlapping trading times of adjacent markets do not necessarily imply natural crossovers. Thus, we follow Bessler and Yang (2003) in establishing three implied volatility timelines: AsiaPacific-Europe-America (ApEA), Europe-America-AsiaPacific (EAAp), and America-Asia/Pacific-Europe (AApE). In ApEA, we assign a timestamp of t to all markets. In EAAp, we assign a timestamp of $t-1$ to American options and a timestamp of t to options in all other regions. Finally, in AApE, we assign a timestamp of $t-1$ to European and American options and a timestamp of t to Asia-Pacific options. In this way, the options markets form natural crossovers globally. These timestamps abide by the fact that Asia-Pacific markets open first, followed by European and American markets. Thus, all time zones can be covered with smooth transitions.

[Insert Figure 2 Here]

4.3. Empirical Implied Volatility Smile

Following Deuskar, Gupta, and Subrahmanyam (2008) and Pena, Rubio, and Serna (1999), we use the quadratic regression method to estimate the structural parameters of the daily implied volatility smiles of index options, as shown in Equation (11).

$$IV = b_0 + b_1 \times \text{Moneyness} + b_2 \times \text{Moneyness}^2, \quad (11)$$

where IV is the Black-Scholes model implied volatility; Moneyness is the ratio between the spot and exercise prices; and the coefficients b_0 , b_1 , and b_2 measure the level, slope, and curvature of the daily volatility smile, respectively. During each trading day, there are about four moneyness and

implied volatility pairs. Hence, we use the cubic spline interpolation suggested by Han, Liang, and Wu (2016) to obtain pairs of options values and their implied volatilities before using Equation (11) to estimate the coefficients b_0 , b_1 , and b_2 .

After we exclude non-trading days, each options market contains 604 implied volatilities over the sample period. Standard augmented Dickey-Fuller tests show that we can reject the null hypothesis of a unit root at the 1% significance level in all markets, satisfying the stationarity requirement of the VAR model. Using the Schwartz information criterion (SIC), we obtain an optimal lag of one for all series. Table 3 reports the coefficients, all of which are significant at the 10% significance level. In particular, the coefficients in the row labeled b_1 are all negative, indicating a downward slope. The coefficients in the row labeled b_2 are positive together with those in b_1 , implying a convex smile curve. The majority of the R^2 and adjusted R^2 values are over 90%, and more than half are over 95%, suggesting that implied volatility smiles exist in most of the options markets.

[Insert Table 3 Here]

5. Aggregated Contagion Analysis

We compute the implied volatility for each market using the method described above, and we use the calculated slopes to set up a standard VAR model. Once we obtain the VAR model, we collect the residuals, and we apply Fisher's Z-statistics to examine the aggregated causal relationships and contagion effects among different options markets.⁶ Figure 3 shows the contagion results from the DAG model for the three constructed time series that are significant at the 5% level. An arrow from one market to another indicates the average spillover from the former to the latter market. The transmission dynamics indicated by the slopes of the implied volatility smiles are clearly complex;

⁶ If a market closes before the opening of another market, no contemporary residuals in the former market should be caused by shocks from the latter market. In addition, the Japanese and Indian markets are both in the Asia-Pacific region, but trading hours overlap for only a short period of time (i.e., about 2.5 hours). Thus, the results regarding these two markets may differ from expectations. For instance, in Figure 3, the Japanese market appears to be disconnected from the other markets, including the other Asia-Pacific markets.

they appear to form interconnected networks and demonstrate strong geographic similarities. The most prominent common feature is that there are two clear clusters: the European and American cluster and the Asia-Pacific cluster. In the first cluster, the U.S. options market consistently triggers implied volatility contagion in other markets, especially many European markets, such as Italy. Switzerland appears to be another dominant market that leads the volatility spillovers. In contrast, Greece seems to be strongly dominated by other markets. The remaining markets primarily have bidirectional volatility spillover effects at different levels. Among these markets, some tend to be affected by contagion but do not cause contagion (e.g., the U.K. and Sweden), while others have more balanced inward and outward contagion impacts (e.g., France). Italy appears to exhibit the opposite behavior from Sweden. The second cluster, which mostly consists of Asia-Pacific options markets, is smaller and less complex. Mainland China dominates the direct or indirect contagion effects on other markets. Thailand has some dominance in contagion, but only in Hong Kong. We categorize Israel as part of the European market, despite its geographical location, because it belongs to many European transnational federations, such as the European Union (EU). Interestingly, Figure 3 shows that Israel falls into the Asia-Pacific cluster rather than the European cluster, and the contagion effects are bidirectional. In this case, Israel's geographic location, rather than its democratic structure, affects its financial connections with other markets. In both clusters, we observe reverse contagion dominance across markets. For instance, the direction of the spillover between Canada and Taiwan, whose trading times do not overlap, reverses in Panel (c). This result may suggest an overnight feedback response from Canada to the existing spillover from Taiwan that occurs early in the day.

[Insert Figure 3 Here]

Although the strong geographic contagion effects that we observe are in line with the findings of Balli, Hajhoj, Basher, and Ghassan (2015) and Baumöhl, Kočenda, Lyócsa, and Výrost (2018), we find that geographically close markets do not necessarily experience contagion clustering. However, we observe a few exceptions. Japan always stands alone from both of the two main

clusters. Australia also tends to stand alone most of the time. This result may occur because both are geographically closer to the Pacific than to Asia and, thus, maintain a fair level of economic independence from other, more Asian markets in this region. In contrast, Taiwan and Korea⁷ appear to primarily cluster with European and American markets rather than with Asia-Pacific markets. Taiwan, for example, has close interconnections with a few markets in the European and American clusters, such as Canada, Brazil, the U.K., and Italy. This finding contradicts the notion of geographic clusters.

As we described previously, the slopes of the implied volatility smile reflect hedging pressure or speculative demand from the spot market. When investors in a market are concerned that the market may drop significantly, their demand for deep out-of-the-money put options increases dramatically. This increase inevitably creates a certain amount of hedging pressure. Figure 3 suggests that such pressure from the U.S. market can spread to the markets in Canada, Switzerland, Greece, the U.K., and Italy directly but does not spread to the markets in Denmark, France, and India. Moreover, the slopes of the implied volatility smiles can also be considered as indicators of a market's future performance. When a market reaches a low point, the slope of the implied volatility tends to be flatter and may often reflect a higher probability that the market will rebound in the future. In Section 6.2, we discuss differences in contagion in different market states in more detail.

6. Time-Varying Spillover Analysis

Our DAG analysis demonstrates that the global options markets tend to smile together. In this section, we first examine contemporary and lagged spillover effects.⁸ In doing so, we aim to overcome the shortcomings of other methods, which require arbitrary prior assumptions on variable

⁷ In Figure 3, Korea appears to connect only to Brazil in Panels (a) and (b), and it appears to stand alone in Panel (c). This result shows that although Korea can be included in the European-American cluster, it weakly connects to the cluster. This result is very different from the result for Taiwan.

⁸ We can consider different lags, such as zero, one, two, three, ten, or thirty days, to measure the market responses to exogenous shocks. In general, we find that cross-spillovers (i.e., exogenous responses) increase and that self-spillovers decrease when the lag is longer (e.g., one versus ten days). Meanwhile, these scenarios may produce similar results because the lags are essentially overcome by the asynchronization stemming from the time zone differences. Thus, we report the contemporary results and the results with a 30-day lag to form clear comparisons.

orderings (Swanson and Granger, 1997)⁹ to obtain robust results. Second, we implement the variance decomposition analysis of the SVAR, which explains the extent to which the estimated variance of the H-day forecasting errors in a specific options market can be ascribed to external shocks in that market or other markets.

6.1. Contemporary and Lagged Spillover Effects

Table 4 reports the results for contemporary and long-run (30-day lag) spillovers in panels (a) and (b), respectively. The number in the i th row and the j th column of the table indicates the percentage of the estimated residuals from the variance decomposition analysis. This value illustrates market j 's response to information shocks from market i . The greater this percentage, the more powerful the cross-spillover or contagion effects (e.g., Diebold and Yilmaz, 2012). The values on the diagonal represent the self-spillover effects within each market. Greater numbers indicate less contagion but stronger self-spillovers in response to shocks. Based on this understanding, the contemporary contagion spillover analysis finds no contagion effects across the majority of markets. This result is demonstrated in two ways. First, for the diagonal values, most of the estimated residuals are 100% (e.g., Australia) or nearly 100% (e.g., Turkey), indicating that information transmission stays within the market itself. Ten markets, including India and Germany, tend to partially contain their responses to shocks internally, but their contagion does not spread to other markets apart from Italy. Second, cross-market reactions to shocks arise in nine markets in Asia-Pacific and Europe, and most of them do not have a high percentage of the residuals apart from Germany (49.7%), India (35.9%), and Denmark (34.8%). On the receiving end, only a handful of markets are affected by contagion effects, and very few of these effects are large (e.g., the Netherlands at 49.7% from Germany and Italy at 35.9% from India). These results are consistent

⁹ For the VAR, the order of the markets that we use is Austria, Australia, Canada, France, Germany, Greece, Hong Kong, the Netherlands, India, Italy, Japan, Korea, Sweden, Switzerland, Taiwan, and the U.S. Table A1 in the appendix presents the constraint matrix A, which corresponds to the DAG results in Figure 3, where the period is a coefficient that must be estimated. Matrix A has 61 such coefficients in total, and matrix B is a 25×25 diagonal unit matrix. The results of estimating the SVAR model are not reported for brevity. Two of the estimated coefficients are significant at the 5% level, whereas the other 59 coefficients are significant at the 1% level.

with our DAG analysis and prior studies of the contemporary contagion effects of implied volatility smile shocks (Morana, 2008).

[Insert Table 4 Here]

However, when markets are given time (e.g., 30 days) to respond to information, we can clearly observe that contagion increases significantly and self-responses fall. First, all of the self-responses decrease over 30 days, and the majority of these decreases are significant (e.g., Japan from 100% to 66.3%, Austria from 100% to 36%, and the U.S. from 100% to 31%). Furthermore, many more markets now exhibit contagion. European markets have the most active bidirectional information responses not only to other European markets but also to international markets. The Asia-Pacific region also experiences a higher level of bidirectional interactions with a 30-day lag than contemporaneously, but more markets in this region seem to be affected by contagion than lead to contagion. The U.S. appears to move from a unidirectional contemporaneous regime (i.e., receiving contagion) to a bidirectional regime, whereas Canada and Brazil show only slight increases in their general information responses without indicating major contagion effects.

We conjecture that the different results of the lagged and contemporaneous tests are due to the fact that the time zones of these global index options markets differ, and it may take time for trading information to be fully reflected in options prices in these markets. Trading frictions and investors' abilities to absorb information may be other explanations for these results.

6.2. Time-Varying Total Spillovers and Directed Spillover Indices

Morana (2008) and Chen, McMillan, and Buckle (2018) suggest that market events, such as financial crises, significantly affect the total volatility of the market. Moreover, spillovers subsequently increase in response to regulatory interventions. Claeys and Vasicek (2012) also suggest that the 2008 liquidity crisis significantly increased the level of spillovers or contagion among assets, which we demonstrate with consistent findings using DAG and total spillover (i.e., both contemporary and lagged) analyses. Thus, we explore the time-varying features of the implied

volatilities in the options markets, especially before and after the 2008 financial crisis¹⁰, by looking at the implied volatility slopes for 16 of the 25 markets in our sample using a 200-day window after applying the SIC. We then conduct a variance decomposition analysis based on a 10-step forward estimation to obtain the total spillover index. This index measures how the responses to shocks in different options markets contribute to the total errors in the variance matrix. In total, we have 2,786 individual-directed outflow spillover indices.

Figure 4 plots the directed spillover index (outflow) with magnitudes for 16 options markets according to Equation (6) in Section 3.2. Taiwan, the U.S., and Switzerland always maintain high levels of outgoing spillovers, whereas Japan, Hong Kong, and India maintain lower levels of these spillovers. One prominent phenomenon in Figure 4 is that multiple markets, including France, Italy, the Netherlands, and Austria, peak on January 20, 2012. However, Germany, Canada, the U.S., and Taiwan valley on that day. This result may be linked to Fitch's announcement downgrading the long-term credit ratings of nine eurozone markets (excluding Greece) on January 13, 2012. The ratings of Italy, Portugal, and Spain were reduced by two grades, those of France and Australia fell by one grade, and those of Germany and Belgium were unchanged. When the market recognized that fundamentals had been impacted in the heavily affected countries, such as France, Italy, and the Netherlands, the hedging pressure from these countries to less affected or non-affected countries started to increase. This result is consistent with Drago and Gallo's (2016) finding that credit ratings can affect financial markets and that downgrades usually cause spillover effects. Furthermore, the scale of the resulting spillover is determined by a country's financial status.

[Insert Figure 4 Here]

The Greek market peaked on May 18, 2012, only one day before both its long- and short-term Fitch credit ratings were degraded from B to CCC and from B to C (the lowest rating), respectively. This downgrading occurred only one month after Fitch changed Greece's rating in April. The change

¹⁰ We exclude nine markets that are relatively new to cover a sufficiently long period prior to the 2008 financial crisis.

was ascribed entirely to the widespread concern that Greece would lose its EU membership. The rates of some of the largest economies in the EU, such as France and Italy, did not suffer from rate downgrading that day. However, the market may have believed that Greece was going to be removed from the EU, further worsening the sovereign debt market in Europe. Thus, we also observe peaks in the implied volatilities of these two markets, providing perfect evidence of spillover effects owing to the growing hedging pressure.

Because Greece's financial stress launched the eurozone sovereign debt crisis, it is essential to examine the outflow spillovers from Greece to understand the full picture of the contagion that spread across almost the entire continent of Europe. Before October 2009, the scale of outflow spillovers from Greece ranged from one to four. Starting on October 20, 2009, when Greece's sovereign debt issue started to emerge, the volatility spillovers of its options market began to increase, peaking at 7.5 on February 7, 2010. Even though the peak fell to an extent, Standard & Poor still downgraded Greece to BB+ on April 27, 2010. The downgrade occurred exactly three days after the Greek government officially asked for financial aid from the EU and the International Monetary Fund. This downgrade forced government intervention immediately, causing Greece's spillover index to increase. Thus, our argument that changes in a country's fundamentals often directly affect its risk exposure, as reflected by the spillover index of the implied volatility smile, is supported.

6.3. Determinants of Volatility Smile Spillovers

The literature (e.g., Han, Liang, and Wu, 2016; Pena, Rubio, and Serna, 1999) suggests that three groups of variables can explain the implied volatility smiles in a market. These groups of variables relate to the benchmark index of the spot market, the options market, and predictors of market trends. We use the same sets of variables to explain the economic determinants of global options market spillovers.¹¹

¹¹ We thank an anonymous reviewer for pointing out that the spillover effects of classic financial factors, such as asset prices, returns, volatilities, jumps, and sentiment, may also determine global options market spillovers. Nevertheless, as we discuss in [Sections 1 and 2](#), the slopes of the implied volatility smiles seem to contain somewhat different information from

The economic indicators used to describe the spot market benchmark include the log returns, trends, and volatility of the market index. The log returns are the daily returns of an index. An increase in the log returns often indicates that the economy has strong fundamentals, which may affect volatility smile spillovers (Drago and Gallo, 2016). The trend in the market index is calculated as the difference between the closing price of the index on the previous day and the closing price 30 days ago. It often indicates the future direction of changes in the index and may influence investors' confidence in the market and, thus, in the level and spillovers of its volatility (Fernandez-Rodríguez, Gomez-Puig, and Sosvilla-Rivero, 2015). The historical volatility of the benchmark index reflects its fluctuations over the past 30 days. A market may experience high volatility during a short period if its fundamentals change significantly, thereby affecting the magnitude of its volatility spillovers.

The implied volatility of ATM options is commonly used to describe options markets. This indicator reflects investors' expectations of the market's future volatility. When it is not fairly constant, spillovers may increase as more information is transmitted. *TermSpread*, the difference between long- and short-term interest rates, is typically used to capture overall market movements and reflect economic cycles. When it increases, the economy expands. However, economic expansion ultimately slows, and the economy eventually contracts. As the economic cycle progresses, the transmission of spillovers from a market to the rest of the world varies accordingly (Bae, Karolyi, and Stulz, 2003). We also introduce *MOVE* and *VIX*, which reflect the widely used Merrill-Lynch Option Volatility Expectations (MOVE) and VIX indices, respectively, as control variables for global risk factors and investors' uncertainty regarding equity and bond prices. *Crisis* and *EuroDebt* are dummy variables. *Crisis* equals one for dates during the 2008 crisis (i.e., from October 12, 2007, to March 5, 2009) and zero otherwise. *EuroDebt* equals one for dates during the eurozone sovereign debt crisis (i.e., from October 12, 2009, to December 31, 2014) and zero otherwise. The regression model is expressed as follows¹²:

these classic factors. Thus, it may be reasonable to suspect that spillovers of volatility smile slopes are not correlated with spillovers of these other factors. We understand that this concern is an empirical issue and choose to address it in a future study.

¹² Descriptive statistics of the variables in Equation (12) are reported in Table A2 in the appendix.

$$SP = \beta_0 + \beta_1 \times Return + \beta_2 \times Trend + \beta_3 \times Volatility + \beta_4 \times ATM + \beta_5 \times TermSpread + \beta_6 \times MOVE + \beta_7 \times VIX + \beta_8 \times Crisis + \beta_9 \times EuroDebt, \quad (12)$$

where SP is the directed spillover index for a particular market. We omit the subscripts for each market i at time t .

Table 5 presents the empirical results for the determinants of directed spillover effects. The first three columns show the results of the regression models without considering individual and time-fixed effects. With the exception of *Return*, all variables have significant effects at the 1% level. The coefficients of *Trend* and *TermSpread* are significantly negative, suggesting that when the economic outlook is gloomier, the implied volatility smile in this market has stronger spillovers to other markets. The coefficients of *ATM* are all significantly negative for the first three regressions, indicating that when investors expect future volatility to fall from a high level, the market has stronger spillovers to other markets. In addition, the results of the third model suggest that during the 2008 financial crisis, the spillover effects of most markets weakened. However, during the eurozone sovereign debt crisis, most market spillovers were enhanced. This finding highlights the different impacts of the two major crises on options market spillovers.

[Insert Table 5 Here]

The results in the fourth column account for 15 dummy variables that reflect the individual fixed effects of the markets. The adjusted R^2 value increases to 0.456, suggesting that non-time-varying factors explain 31.1% of the changes in the spillovers. We conduct a robustness check on the individual markets' fixed effects and obtain a χ^2 value of 24,000, with a p -value of 0.000. This result suggests that the individual fixed effects are significant.

In the fifth model, we explicitly control for time effects. The χ^2 value is 176, with a p -value of 0.00. Thus, even if we control for both the 2008 financial crisis and the eurozone debt crisis, the spillovers of different markets vary significantly over time. However, the adjusted R^2 value

increases by only 2% compared with the fourth model, implying that these time effects do not significantly explain the spillovers from individual markets.

7. Conclusions

The classic VAR and variance decomposition methods and Granger causality models face several limitations. Thus, we propose a network approach to analyze the contagion effects among global index options markets. Once this flexible method confirms the existence of contagion, we comprehensively study contemporaneous, lagged, and time-varying volatility spillover effects. To better understand these complex dynamics, we compute both the total and directed spillover indices with a forecasting view of the global options markets. In this way, we can robustly confirm that the individual options markets within this system transmit information in the form of network contagion and clustering, often more organically and in line with the economic links between countries. For instance, the DAG results clearly identify two clusters, Europe-America and Asia-Pacific, each covering markets across a wide geographic range.

Most options markets tend to be self-contained, as the contemporary spillover effects indicate. However, when we introduce a lag of 30 days, this independence declines, and strong connections among countries emerge. In particular, Europe appears to be a highly active region with strong bidirectional transmissions of volatilities, which makes sense in that European countries have historically been closely economically tied. Another interesting result is that the U.S. seems to be more exogenous in the contemporaneous results, but it triggers and is influenced by contagion effects when we include a 30-day lag. Finally, we find that volatility spillovers tend to affect many Asian countries and regions.

We also highlight that index options markets worldwide tend to interact well, even during various crisis periods. Often, spillover effects are greatly amplified during crisis periods but shrink (not necessarily to pre-crisis levels) after a crisis ends. Different markets also experience volatility spillovers to different extents, and these differences are commonly connected to changes in the fundamentals of each economy.

Finally, short-run fluctuations in the underlying index, the volatility implied by ATM options,

and the term spreads of interest rates are key determinants of volatility spillovers.

References

- Abdul-Rahim, R., Sopian, R. Z., & Mohd Nor, A. H. S. (2008). Stocks market interdependence and Asian financial crisis: Empirical evidence from Asean-Plus-Three. *Journal of Muamalat and Islamic Finance Research*, 5(1), 95-112.
- Awokuse, T. O. (2006). Export-led growth and the Japanese economy: Evidence from VAR and directed acyclic graphs. *Applied Economics*, 38(5), 593-602.
- Bae, K.-H., Karolyi, G. A., & Stulz, R. M. (2003). A new approach to measuring financial contagion. *Review of Financial Studies*, 16(3), 717-763.
- Bakshi, G., Cao, C., & Chen, Z. (2000). Do call prices and the underlying stock always move in the same direction? *Review of Financial Studies*, 13(3), 549-584.
- Balli, F., Hajhoj, H. R., Basher, S. A., & Ghassan, H. B. (2015). An analysis of returns and volatility spillovers and their determinants in emerging Asian and Middle Eastern countries. *International Review of Economics and Finance*, 39, 311-325.
- Baruník, J., Kočenda, E., & Vácha, L. (2016). Asymmetric connectedness on the US stock market: Bad and good volatility spillovers. *Journal of Financial Markets*, 27, 55-78.
- Baumöhl, E., Kočenda, E., Lyócsa, S., & Výrost, T. (2018). Networks of volatility spillovers among stock markets. *Physica A: Statistical Mechanics and Its Applications*, 490, 1555-1574.
- Bessler, D. A., & Loper, N. (2001). Economic development: Evidence from directed acyclic graphs. *The Manchester School*, 69(4), 457-476.
- Bessler, D. A., & Yang, J. (2003). The structure of interdependence in international stock markets. *Journal of International Money and Finance*, 22(2), 261-287.
- Bollen, N. P. B., & Whaley, R. E. (2004). Does net buying pressure affect the shape of implied volatility functions? *Journal of Finance*, 59(2), 711-753.
- Boyer, B. H., Kumagai, T., & Yuan, K. (2006). How do crises spread? Evidence from accessible and inaccessible stock indices. *Journal of Finance*, 61(2), 957-1003.

- Briere, M., Chapelle, A., & Szafarz, A. (2012). No contagion, only globalization and flight to quality. *Journal of International Money and Finance*, 31(6), 1729-1744.
- Chan, K. C., Cheng, L. T. W., & Lung, P. (2004). Net buying pressure, volatility smile, and abnormal profit of Hang Seng index options. *Journal of Futures Markets*, 24(12), 1165-1194.
- Chan-Lau, J. A., Mathieso, D. J., & Yao, J. Y. (2004). Extreme contagion in equity markets. *IMF Staff Papers*, 51(2), 386-408.
- Chang, R., & Majnoni, G. (2002). Fundamentals, beliefs, and financial contagion. *European Economic Review*, 46(4-5), 801-808.
- Chen, J., McMillan, D., & Buckle, M. (2018). Information transmission across European equity markets during crisis periods. *The Manchester School*, 86(6), 770-788.
- Chou, R. K., Chung, S.-L., Hsiao, Y.-J., & Wang, Y.-H. (2011). The impact of liquidity on option prices. *Journal of Futures Markets*, 31(12), 1116-1141.
- Claeys, P., & Vašíček, B. (2014). Measuring bilateral spillover and testing contagion on sovereign bond markets in Europe. *Journal of Banking & Finance*, 46, 151-165.
- Connolly, R. A., & Wang, F. A. (2003). International equity market comovements: Economic fundamentals or contagion? *Pacific-Basin Finance Journal*, 11(1), 23-43.
- Corsetti, G., Pericoli, M., & Sbracia, M. (2005). 'Some contagion, some interdependence': More pitfalls in tests of financial contagion. *Journal of International Money and Finance*, 24(8), 1177-1199.
- Daly, K., Batten, J.A., Mishra, A.V. & Choudhury, T. (2019). Contagion risk in global banking sector. *Journal of International Financial Markets, Institutions and Money*, 63, 101136.
- Deuskar, P., Gupta, A., & Subrahmanyam, M. G. (2008). The economic determinants of interest rate option smiles. *Journal of Banking & Finance*, 32(5), 714-728.
- Diebold, F. X., & Yilmaz, K. (2009). Measuring financial asset return and volatility spillovers, with application to global equity markets. *Economic Journal*, 119(534), 158-171.
- Diebold, F. X., & Yilmaz, K. (2012). Better to give than to receive: Predictive directional measurement of volatility spillovers. *International Journal of Forecasting*, 28(1), 57-66.

- Drago, D., & Gallo, R. (2016). The impact and the spillover effect of a sovereign rating announcement on the euro area CDS market. *Journal of International Money and Finance*, 67, 264-286.
- Duan, J.-C., & Wei, J. (2009). Systematic risk and the price structure of individual equity options. *Review of Financial Studies*, 22(5), 1981-2006.
- Eraker, B., Johannes, M., & Polson, N. (2003). The impact of jumps in volatility and returns. *Journal of Finance*, 58(3), 1269-1300.
- Eun, C. S., & Shim, S. (1989). International transmission of stock market movements. *Journal of Financial and Quantitative Analysis*, 24(2), 241-256.
- Fernandez-Rodríguez, F., Gomez-Puig, M. & Sosvilla-Rivero, S. (2015). Volatility spillovers in EMU sovereign bond markets. *International Review of Economics and Finance*, 39, 337-352.
- Finta, M. A., & Aboura, S. (2020). Risk premium spillovers among stock markets: Evidence from higher-order moments. *Journal of Financial Markets*, 49, 100533.
- Forbes, K. J., & Rigobon, R. (2002). No contagion, only interdependence: Measuring stock market comovements. *Journal of Finance*, 57(5), 2223-2261.
- Friesen, G. C., Zhang, Y., & Zorn, T. S. (2012). Heterogeneous beliefs and risk neutral skewness. *Journal of Financial and Quantitative Analysis*, 47(4), 851-872.
- Garleanu, N., Pedersen, L. H., & Poteshman, A. M (2009). Demand-based option pricing. *Review of Financial Studies*, 22(10), 4259-4299.
- Gemmill, G., & Kamiyama, N. (2000). International transmission of option volatility and skewness: When you're smiling, does the whole world smile? City University Business School, London, working paper (May 2000).
- Greenwood-Nimmo, M., Nguyen, V. H., & Rafferty, B. (2016). Risk and return spillovers among the G10 currencies. *Journal of Financial Markets*, 31, 43-62.
- Gulko, L. (2002). Decoupling. *Journal of Portfolio Management*, 28(3), 59-66.
- Hamao, Y., Masulis, R. W., & Ng, V. (1990). Correlations in price changes and volatility across international stock markets. *Review of Financial Studies*, 3(2), 281-307.

- Han, B. (2008). Investor sentiment and option prices. *Review of Financial Studies*, 21(1), 387-414.
- Han, Q., Liang, J., & Wu, B. (2016). Cross economic determinants of implied volatility smile dynamics: Three major European currency options. *European Financial Management*, 22(5), 817-852.
- Hull, J., & White, A. (1987). The pricing of options on assets with stochastic volatilities. *Journal of Finance*, 42(2), 281-300.
- Kim, S.-J., Moshirian, F., & Wu, E. (2006). Evolution of international stock and bond market integration: Influence of the European Monetary Union. *Journal of Banking & Finance*, 30(5), 1507-1534.
- Kim, J. S., & Ryu, D. (2015). Are the KOSPI 200 implied volatilities useful in value-at-risk models? *Emerging Markets Review*, 22, 43-64.
- Kim, J. S., Ryu, D., & Seo, S. W. (2015). Corporate vulnerability index as a fear gauge? Exploring the contagion effect between U.S. and Korean markets. *Journal of Derivatives*, 23(1), 73-88.
- Koop, G., Pesaran, M. H., & Potter, S. M. (1996). Impulse response analysis in nonlinear multivariate models. *Journal of Econometrics*, 74(1), 119-147.
- Koutmos, G., & Booth, G. G. (1995). Asymmetric volatility transmission in international stock markets. *Journal of International Money and Finance*, 14(6), 747-762.
- Lin, W.-L., Engle, R. F., & Ito, T. (1994). Do bulls and bears move across borders? International transmission of stock returns and volatility. *Review of Financial Studies*, 7(3), 507-538.
- Masson, P. (1999). Contagion: Macroeconomic models with multiple equilibria. *Journal of International Money and Finance*, 18(4), 587-602.
- Morana, C. (2008). International stock markets comovements: The role of economic and financial integration. *Empirical Economics*, 35(2), 333-359.
- Morris, S., & Shin, H. S. (2000). Rethinking multiple equilibria in macroeconomic modeling. *NBER Macroeconomics Annual*, 15, 139-161.

- Narwal, K., Sheera, V., & Mittal, R. (2012). Spillovers and transmission in emerging and mature markets implied volatility indices. *International Journal of Financial Management*, 2(4), 47-59.
- Pearl, J. (1995). Causal diagrams for empirical research. *Biometrika*, 82(4), 669-688.
- Pena, I., Rubio, G., & Serna, G. (1999). Why do we smile? On the determinants of the implied volatility function. *Journal of Banking & Finance*, 23(8), 1151-1179.
- Pesaran, H. H., & Shin, Y. (1998). Generalized impulse response analysis in linear multivariate models. *Economics Letters*, 58(1), 17-29.
- Ryu, D., Kang, J., & Suh, S. (2015). Implied pricing kernels: An alternative approach for option valuation. *Journal of Futures Markets*, 35(2), 127-147.
- Ryu, D., Ryu, D., & Yang, H. (2021). The impact of net buying pressure on index options prices. *Journal of Futures Markets*, 41(1), 27-45.
- Ryu, D., Webb, R. I., Yang, H., & Yu, J. (2022). Investors' net buying pressure and implied volatility dynamics. *Borsa Istanbul Review*, Forthcoming.
- Ryu, D., & Yang, H. (2022). Intraday option price changes and net buying pressure. *Applied Economics Letters*, Forthcoming.
- Sewraj, D., Gebka, B., & Anderson, R. D. J. (2018). Identifying contagion: A unifying approach. *Journal of International Financial Markets, Institutions and Money*, 55, 224-240.
- Shu, H.-C., & Chang, J.-H. (2019). Spillovers of volatility index: Evidence from U.S., European, and Asian stock markets. *Applied Economics*, 51(19), 2070-2083.
- Sim, M., Ryu, D., & Yang, H. (2016). Tests on the monotonicity properties of KOSPI 200 options prices. *Journal of Futures Markets*, 36(7), 625-646.
- Spirtes, P., Glymour, C., & Scheines, R. (2000). Causation, prediction, and search. *MIT Press*.
- Swanson, N. R., & Granger, C. W. J. (1997). Impulse response functions based on a causal approach to residual orthogonalization in vector autoregressions. *Journal of the American Statistical Association*, 92(437), 357-367.
- Van Rijckeghem, C., & Weder, B. (2001). Sources of contagion: Is it finance or trade? *Journal of International Economics*, 54(2), 293-308.

- Worthington, A., & Higgs, H (2004). Transmission of equity returns and volatility in Asian developed and emerging markets: A multivariate GARCH analysis. *International Journal of Finance & Economics*, 9(1), 71-80
- Yang, J., & Bessler, D. A. (2004). The international price transmission in stock index futures markets. *Economic Inquiry*, 42(3), 370-386.
- Yang, H., Choi, H.-S., & Ryu, D. (2017). Option market characteristics and price monotonicity violations. *Journal of Futures Markets*, 37(5), 473-498.
- Yang, J., & Zhou, Y. (2013). Credit risk spillovers among financial institutions around the global credit crisis: Firm-level evidence. *Management Science*, 59(10), 2343-2359.

Appendix A. Correlation Matrix Analysis

The error terms of vector autoregressions (VARs) reflect information that is not captured in historical data. Furthermore, their pairwise correlations indicate the degree to which each pair of options markets is affected by information shocks on the same trading day.

Table A1 reports the correlation matrix of the VAR model. We find that if two options markets are located on geographically different continents, they tend to have a low correlation. In contrast, markets in the same geographic region are highly correlated. For example, Germany and the Netherlands have the highest correlation coefficient of 0.72. Next, Denmark and Switzerland, Italy and Denmark, and Sweden and Switzerland have correlation coefficients of 0.70, 0.67, and 0.66, respectively. In contrast, Thailand and Austria, Brazil and Turkey, and Canada and Denmark have correlation coefficients that are close to zero. Van Rijckeghem and Weder (2001) and Abdul-Rahim, Sopian, and Mohd Nor (2008) point out that the more economic links two countries share, the more correlated their financial markets, including their options markets, are. Our results corroborate these findings. For example, the markets in EU countries are clearly more correlated, consistent with Han, Liang, and Wu (2016). In contrast, their correlations with their non-EU counterparts are much smaller. For example, Norway, Italy, and Denmark are EU countries in the same time zone. Norway and Denmark have a correlation of -0.04, whereas Italy and Denmark have a correlation of 0.67.

However, we acknowledge that the correlations of countries with high and low correlations are very different. This result may be largely due to the time asynchronization across markets, especially markets located on different continents. The Taiwanese and Japanese markets are exceptions. These markets have low correlations with other markets (<0.1), perhaps because their electronic trading platforms run continuously and synchronize with other markets in sequence.

Table A1. Correlation Matrix

This table reports the correlations among all the index options included in this study.

| | AT | AU | BR | CA | CN | DK | FR | DE | GR | HK | NL | IN | IL | IT | JP | KR | NO | RU | SE | CH | TH | TR | TW | UK | US |
|----|------|------|------|------|------|------|------|------|------|------|------|------|------|------|------|------|------|------|------|------|------|------|------|------|------|
| AT | 1.00 | | | | | | | | | | | | | | | | | | | | | | | | |
| AU | - | 1.00 | | | | | | | | | | | | | | | | | | | | | | | |
| BR | - | 0.05 | 1.00 | | | | | | | | | | | | | | | | | | | | | | |
| CA | - | 0.08 | - | 1.00 | | | | | | | | | | | | | | | | | | | | | |
| CN | - | - | - | - | 1.00 | | | | | | | | | | | | | | | | | | | | |
| DK | - | - | - | 0.00 | - | 1.00 | | | | | | | | | | | | | | | | | | | |
| FR | 0.03 | - | 0.08 | - | 0.01 | 0.58 | 1.00 | | | | | | | | | | | | | | | | | | |
| DE | 0.23 | - | 0.09 | 0.06 | 0.00 | - | 0.15 | 1.00 | | | | | | | | | | | | | | | | | |
| GR | 0.09 | 0.11 | - | 0.11 | - | 0.40 | 0.04 | - | 1.00 | | | | | | | | | | | | | | | | |
| HK | 0.01 | - | - | - | 0.12 | 0.00 | 0.03 | 0.00 | - | 1.00 | | | | | | | | | | | | | | | |
| NL | 0.35 | - | 0.14 | 0.02 | - | - | 0.16 | 0.72 | - | 0.02 | 1.00 | | | | | | | | | | | | | | |
| IN | 0.01 | - | - | 0.00 | 0.15 | 0.01 | 0.04 | - | - | 0.33 | 0.00 | 1.00 | | | | | | | | | | | | | |
| IL | 0.04 | - | 0.00 | 0.02 | 0.28 | 0.01 | 0.04 | 0.02 | - | 0.29 | 0.02 | 0.61 | 1.00 | | | | | | | | | | | | |
| IT | 0.11 | - | 0.04 | 0.08 | 0.00 | 0.67 | 0.59 | 0.02 | 0.40 | 0.01 | 0.00 | 0.04 | 0.05 | 1.00 | | | | | | | | | | | |
| JP | - | 0.01 | 0.06 | 0.04 | - | - | - | - | 0.00 | - | - | 0.00 | 0.01 | - | 1.00 | | | | | | | | | | |
| KR | - | 0.04 | 0.13 | 0.02 | - | 0.04 | 0.08 | - | - | - | 0.03 | - | - | 0.06 | - | 1.00 | | | | | | | | | |
| NO | 0.03 | 0.07 | 0.07 | 0.03 | - | - | - | 0.00 | - | - | 0.06 | - | 0.01 | - | 0.01 | 0.01 | 1.00 | | | | | | | | |
| RU | - | - | 0.02 | - | 0.01 | 0.10 | 0.15 | 0.02 | - | 0.04 | 0.06 | 0.03 | 0.03 | 0.05 | 0.03 | - | - | 1.00 | | | | | | | |
| SE | - | 0.01 | 0.04 | 0.11 | 0.00 | 0.60 | 0.56 | - | 0.38 | 0.01 | - | 0.03 | 0.01 | 0.61 | - | 0.09 | - | 0.03 | 1.00 | | | | | | |
| CH | - | 0.04 | 0.06 | 0.11 | - | 0.70 | 0.47 | - | 0.49 | 0.01 | - | 0.03 | 0.03 | 0.62 | - | 0.06 | 0.01 | 0.04 | 0.66 | 1.00 | | | | | |
| TH | 0.00 | - | - | - | 0.02 | - | - | 0.00 | - | 0.30 | - | 0.05 | 0.00 | - | - | 0.00 | - | 0.04 | - | - | 1.00 | | | | |
| TR | 0.05 | - | 0.00 | - | - | - | - | - | - | - | 0.03 | - | - | - | 0.02 | 0.01 | 0.15 | - | - | - | - | 1.00 | | | |
| TW | 0.04 | 0.03 | 0.13 | 0.16 | - | 0.01 | 0.05 | 0.08 | - | - | 0.07 | 0.00 | 0.00 | 0.01 | 0.01 | 0.01 | 0.07 | - | 0.04 | 0.05 | - | 0.06 | 1.00 | | |
| UK | 0.03 | 0.04 | 0.05 | 0.09 | 0.01 | 0.55 | 0.41 | - | 0.48 | 0.00 | - | 0.03 | 0.02 | 0.54 | - | 0.10 | - | 0.07 | 0.62 | 0.61 | - | - | 0.10 | 1.00 | |
| US | 0.04 | 0.08 | 0.02 | 0.16 | - | 0.36 | 0.19 | - | 0.40 | - | - | 0.00 | 0.01 | 0.42 | - | 0.05 | 0.00 | 0.07 | 0.51 | 0.50 | - | - | 0.00 | 0.50 | 1.00 |

Table A2. Descriptive Statistics

This table reports descriptive statistics of the variables for the global index options markets.

| Variables | Sample size | Mean | Medium | Std. | Skew. | Kurt. | Min. | Max. |
|------------|-------------|----------|----------|----------|-------|--------|----------|----------|
| Return | 44,576 | 2.18E-05 | 9.85E-05 | 0.01 | -0.31 | 12.35 | -0.08 | 0.07 |
| Trend | 44,576 | 1.73E-03 | 0.01 | 0.08 | -1.06 | 7.66 | -0.68 | 0.41 |
| Volatility | 44,576 | 4.22E-03 | 2.40E-03 | 5.24E-05 | 2.95 | 13.01 | 2.40E-04 | 3.88E-02 |
| ATM | 44,576 | 22.26 | 18.62 | 13.61 | 5.48 | 107.88 | 0.45 | 477.35 |
| TermSpread | 43,184 | 1.95 | 0.53 | 7.34 | 7.09 | 55.37 | -2.43 | 65.17 |
| MOVE | 44,576 | 88.36 | 78.94 | 33.53 | 1.65 | 6.18 | 43.97 | 264.6 |
| VIX | 44,576 | 19.8 | 17.01 | 9.66 | 2.34 | 10.31 | 9.14 | 80.86 |

Appendix B. Specification of the PC Algorithm

In the global index options directed acyclic graph (DAG), each of the 25 individual markets is represented by a node (see Section 4). We use the slopes of the individual implied volatility smiles to set up the VAR models (see Equation 1). We collect the residuals from the VARs, which are conditional variances, and use them as edges in the DAG. In theory, each node is connected to the other 24 nodes, and we use the PC algorithm to determine the directed edges between the pairs of nodes. The first stage in this process is the elimination, which removes edges between pairs of variables that have zero correlation. For the remaining edges, the algorithm examines first-order partial correlations (the correlations between the pairs conditional on a third variable) using Fisher's Z -statistics. If this correlation is zero for a given pair of nodes, that pair is eliminated from the graph; otherwise, the search continues until conditional correlation is achieved. The maximum search that the algorithm may reach is $N-2=23$.

After this elimination process, the PC algorithm proceeds to the orientation process, which assigns the directions of the contemporaneous causal flows among the remaining nodes using subsets. According to Yang and Zhou (2013), "the subset of a pair of variables whose edge has been removed is the conditioning variable(s) on the removed edge between two variables." This process removes nodes that have vanishing zero-order conditional or unconditional correlations and keeps the rest, which can be connected with directed edges. Eventually, the algorithm builds a cyclic graph through a full circle of directed causal flows, which visually illustrates such features as the connectivity and centrality among the nodes in the network.

Figure 1. Time-varying Slopes and Levels of Implied Volatility Smiles

Figure 1 shows the time series for the levels and slopes of the implied volatilities of index options in the U.S., Germany, Japan, and India. The black (gray) line indicates the time-series process for the level (slope) of each index options implied volatility. As the figure shows, the variance of the slope is much higher than that of the level in all four markets.

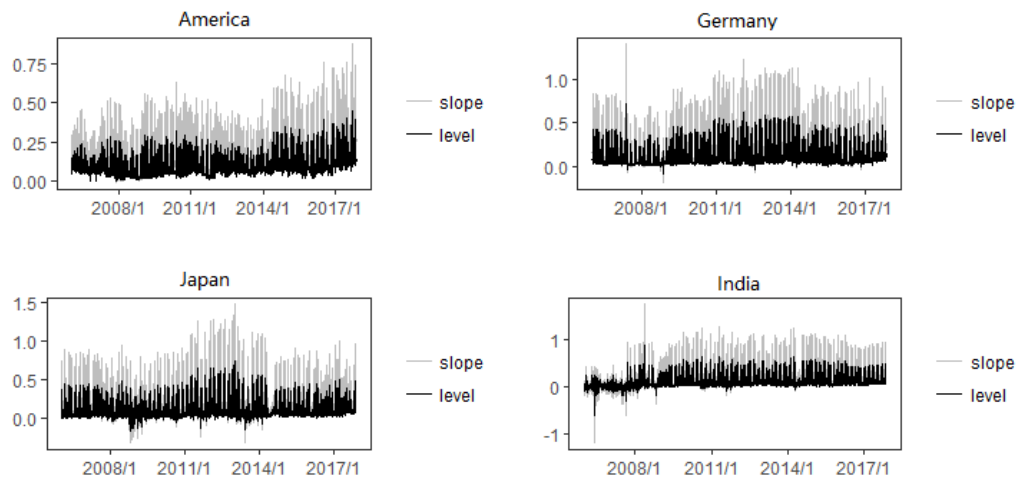


Figure 2. Trading Times of Global Options Markets

Figure 2 reports the opening and closing hours for each index options market in the sample. All times are adjusted to the Beijing time zone. The trading times in these markets overlap in multiple instances, suggesting that we need to consider ways to group them according to a certain sequence of trading times.

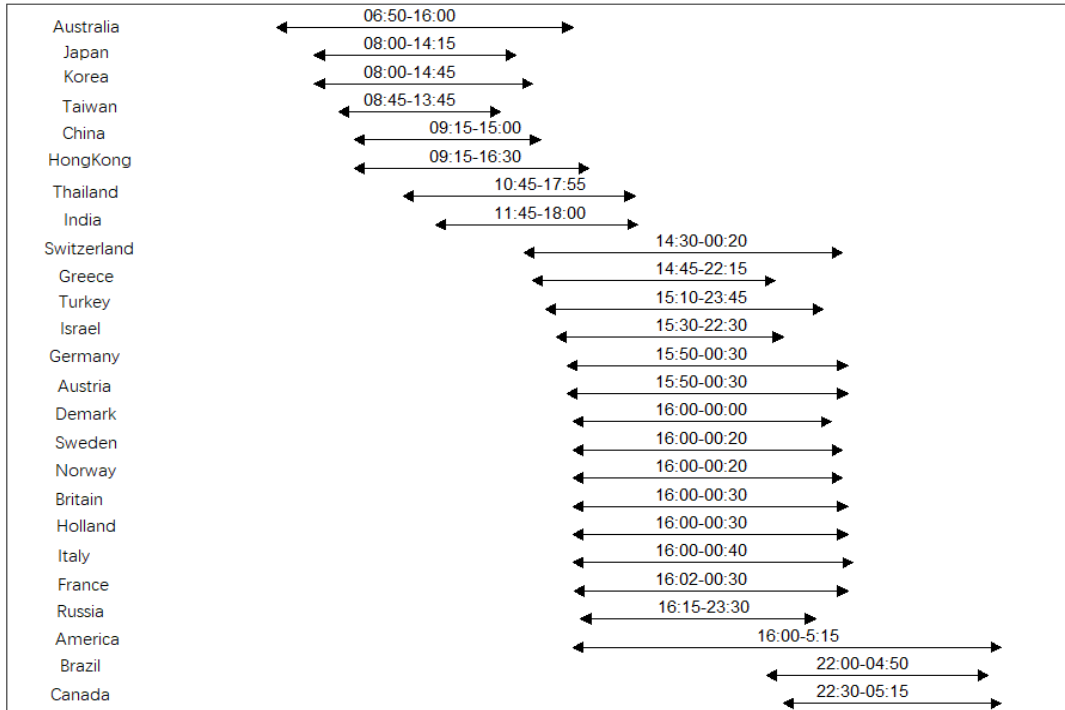
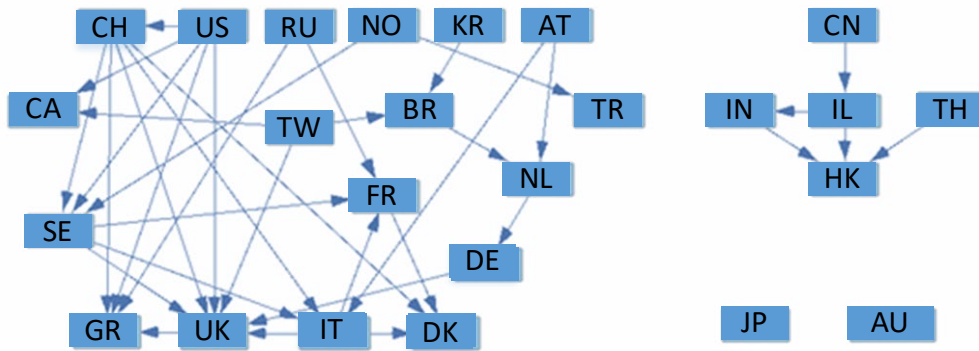


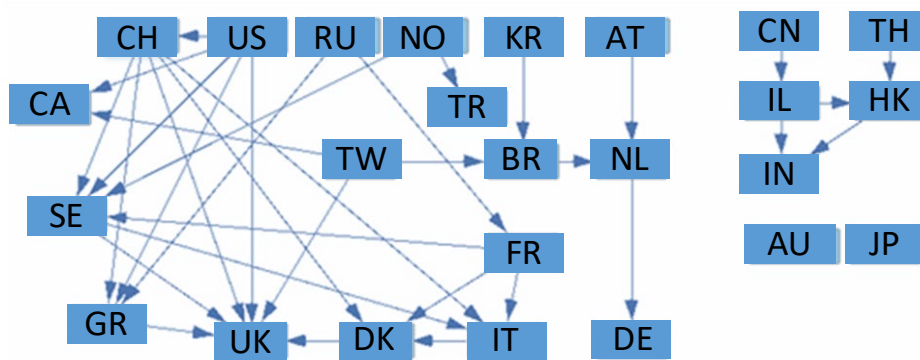
Figure 3. Directed Acyclic Graph Results for Three Global Time Series

Figure 3 illustrates the aggregated contagion results from the DAG model for the three constructed time series. We illustrate significant results at the 5% level. An arrow from market A to market B indicates the average spillover from market A to market B.

Panel (a): AsiaPacific-Europe-America (ApEA) Series



Panel (b): Europe-America-AsiaPacific (EAAp) Series



Panel (c): America-AsiaPacific-Europe (AApE) Series

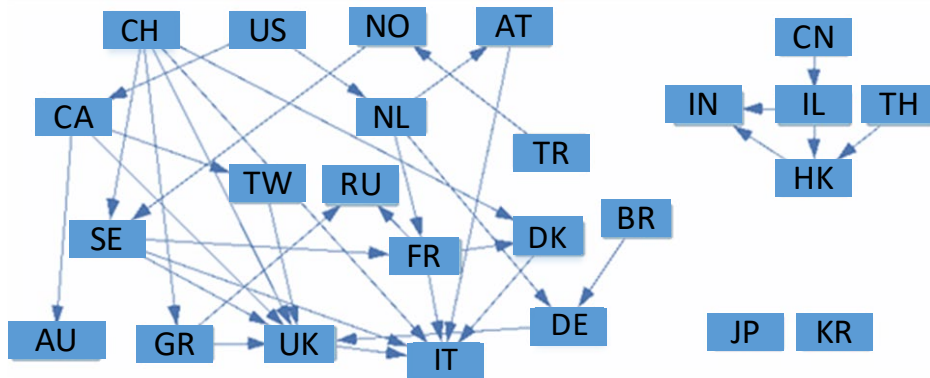


Figure 4. Directed Outflow Spillovers of the Implied Volatility Smiles from Global Options Markets

Figure 4 plots a directed spillover (outflow) index with magnitudes for 16 options markets using Equation (6) in Section 3.2:

$$S^g(H) = \frac{\sum_{i,j=1, i \neq j}^n \bar{\theta}_{ij}^g(H)}{\sum_{i,j=1}^n \bar{\theta}_{ij}^g(H)} \times 100 = \frac{\sum_{i,j=1, i \neq j}^n \bar{\theta}_{ij}^g(H)}{N} \times 100. \text{ Taiwan, the U.S., and Switzerland maintain high outflow spillovers}$$

throughout the sample period, whereas Japan, Hong Kong, and India maintain lower levels of spillovers.

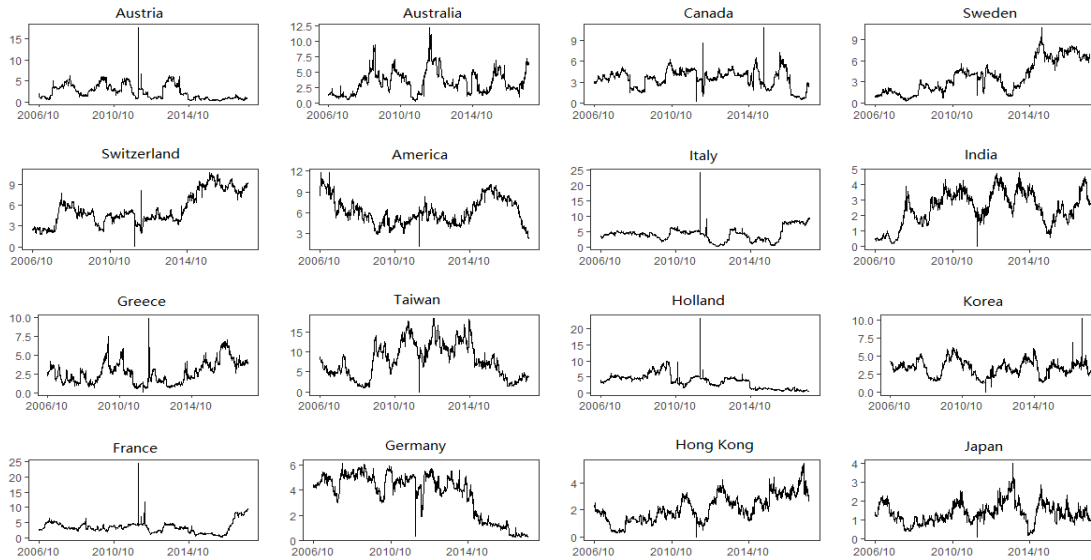


Table 2. Descriptive Statistics

This table reports descriptive statistics for each index options market. The markets are organized into three continents: Asia-Pacific, America, and Europe. *No. Obs.*, *Mean*, *Median*, *Std.*, *Skewness*, *Kurtosis*, *Min.*, and *Max.* denote the number of observations (i.e., the sample size) and the sample mean, median, standard deviation, skewness, kurtosis, minimum, and maximum values, respectively. The market codes are given in Table 1.

| Market | <u>Asia-Pacific</u> | | | | | | | | <u>America</u> | | | | | |
|-----------------|---------------------|--------|--------|--------|--------|--------|--------|--------|----------------|--------|--------|--------|---------|--------|
| | AU | JP | KR | TW | CN | HK | TH | IN | US | CA | BR | | | |
| No. Obs. | 12,592 | 11,636 | 11,732 | 11,672 | 2,684 | 11,692 | 9,800 | 11,676 | 12,936 | 12,492 | 2,380 | | | |
| Mean | 23.29 | 28.02 | 24.85 | 24.24 | 27.51 | 27.21 | 24.53 | 27.86 | 21.33 | 26.97 | 27.35 | | | |
| Median | 20.13 | 24.94 | 21.27 | 21 | 24.26 | 22.62 | 22.47 | 23.96 | 18.92 | 22.08 | 26.36 | | | |
| Std. | 13.09 | 12.42 | 13.27 | 11.85 | 14.74 | 14.69 | 12.44 | 13.74 | 10.7 | 21.09 | 7.23 | | | |
| Skewness | 2.6 | 1.97 | 2.08 | 1.55 | 1.42 | 2.42 | 2.46 | 1.7 | 1.69 | 6.34 | 1.15 | | | |
| Kurtosis | 13.25 | 8.45 | 8.66 | 5.8 | 5.83 | 13.21 | 15.45 | 6.88 | 7.29 | 87.43 | 7.1 | | | |
| Min. | 3.63 | 5.69 | 5.84 | 6.05 | 5.3 | 4.26 | 4.05 | 1.25 | 3.61 | 5.09 | 12.61 | | | |
| Max. | 141.01 | 117.03 | 116.36 | 87.47 | 110.57 | 195.18 | 210.05 | 131.99 | 97.51 | 504.16 | 95.28 | | | |
| Market | <u>Europe</u> | | | | | | | | | | | | | |
| | CH | GR | TR | IL | DE | AT | DK | SE | NO | UK | NL | IT | FR | RU |
| No. Obs. | 11,924 | 11,708 | 3,892 | 9,428 | 12,044 | 11,850 | 3,864 | 12,492 | 3,096 | 10,240 | 12,088 | 12,636 | 12,144 | 5,508 |
| Mean | 22.34 | 43.03 | 26.23 | 21.93 | 26.41 | 27.37 | 20.74 | 27.6 | 22.14 | 23.13 | 26.6 | 30.38 | 27.08 | 33.14 |
| Median | 19.65 | 40.79 | 23.97 | 20.09 | 23.37 | 24.72 | 18.78 | 24.17 | 20.16 | 20.98 | 22.62 | 26.25 | 23.73 | 29.9 |
| Std. | 10.96 | 19.52 | 11.3 | 9.21 | 12.51 | 14.71 | 8.16 | 14.37 | 21.07 | 11.37 | 20.35 | 24.02 | 16.03 | 15.96 |
| Skewness | 1.94 | 1.6 | 5.51 | 1.18 | 2.07 | 8.21 | 2.23 | 2.14 | 40.04 | 2.12 | 9.79 | 11.91 | 6.32 | 6.61 |
| Kurtosis | 8.72 | 9.81 | 57.11 | 4.61 | 10.76 | 132.08 | 11.52 | 10.56 | 1,934.25 | 11.97 | 155.9 | 215.09 | 80.33 | 80.32 |
| Min. | 3.76 | 6.94 | 9.5 | 4.71 | 7.06 | 0.91 | 8.96 | 5.04 | 8.66 | 5.81 | 5.19 | 4.21 | 0.45 | 0.93 |
| Max. | 120.25 | 245.89 | 218.43 | 71.23 | 164.33 | 381.6 | 93.12 | 154.98 | 1,062.60 | 143.46 | 399.65 | 618.48 | 273.944 | 261.77 |

Table 3. Empirical Implied Volatility Smiles

This table presents the coefficients describing the level, slope, and curvature of the daily volatility smile with b_0 , b_1 , and b_2 , respectively for each market. The numbers in parentheses are standard errors. The coefficient b_0 reflects the level of the daily volatility smile. The coefficient b_1 indicates the downward slope of the volatility smile. The coefficient b_2 measures the smile's curvature. The coefficient estimates are statistically significant at the 10% level. The majority of the R^2 and adjusted R^2 values are over 90%, and more than half are over 95%, suggesting that implied volatility smiles exist in most options markets.

| Market | <u>Asia-Pacific</u> | | | | | | | | <u>America</u> | | | | | |
|------------------------------|------------------------|-----------------------|-----------------------|-----------------------|-----------------------|------------------------|------------------------|------------------------|-----------------------|------------------------|-----------------------|-----------------------|-----------------------|---------------------|
| | AU | JP | KR | TW | CN | HK | TH | IN | US | CA | BR | | | |
| b_0 | 756.34 (-54.36) | 804.87 (-40.79) | 650.76 (-34.78) | 760.55 (-26.82) | 736.75 (-41.91) | 699.98 (-27.30) | 437.33 (-62.17) | 817.79 (-46.05) | 785.75 (-40.32) | 1,226.24 (-66.07) | 365.36 (-19.20) | | | |
| b_1 | -1,572.15 (-108.76) | -1,663.12 (-81.61) | -1,350.33 (-69.59) | -1,562.11 (-53.66) | -1,494.11 (-83.86) | -1,447.24 (-54.62) | -903.57 (-124.39) | -1,676.14 (-92.12) | -1,650.02 (-80.66) | -2,536.76 (-132.18) | -774.08 (-38.41) | | | |
| b_2 | 833.85 (-54.25) | 880.95 (-40.70) | 720.07 (-34.71) | 820.90 (-26.77) | 780.38 (-41.83) | 769.83 (-27.25) | 487.82 (-62.04) | 880.96 (-45.95) | 879.97 (-40.23) | 1,329.22 (-65.93) | 433.41 (-19.16) | | | |
| R^2 | 0.94 | 0.95 | 0.94 | 0.98 | 0.89 | 0.97 | 0.82 | 0.94 | 0.98 | 0.96 | 0.97 | | | |
| Adj. R^2 | 0.94 | 0.94 | 0.94 | 0.98 | 0.88 | 0.97 | 0.82 | 0.94 | 0.98 | 0.96 | 0.97 | | | |
| - | <u>Europe</u> | | | | | | | | | | | | | |
| Market | CH | GR | TR | IL | DE | AT | DK | SE | NO | UK | NL | IT | FR | RU |
| b_0 | 792.75 (-47.51) | 246.10 (-69.13) | 460.10 (-74.23) | 830.19 (-41.29) | 775.67 (-42.51) | 547.06 (-93.60) | 586.25 (-51.94) | 870.99 (-52.98) | 96.51 (-49.91) | 638.99 (-52.04) | 986.28 (-47.32) | 978.37 (-30.50) | 759.67 (-42.63) | 332.16 (-36.23) |
| b_1 | -1,650.95 (-95.05) | -488.90 (-138.31) | -955.54 (-148.50) | -1,710.36 (-82.60) | -1,623.52 (-85.06) | -1,142.78 (-187.26) | -1,226.16 (-103.91) | -1,811.29 (-106.00) | -245.18 (-99.86) | -1,358.47 (-104.11) | -2,039.01 (-94.67) | -2,011.36 (-61.01) | -1,591.94 (-85.28) | -702.56 (-72.48) |
| b_2 | 875 (-47.41) | 284.54 (-68.99) | 518.60 (-74.07) | 896.60 (-41.20) | 868.76 (-42.42) | 619.02 (-93.40) | 656.42 (-51.83) | 961.93 (-52.87) | 169.57 (-49.81) | 737.72 (-51.93) | 1,072.70 (-47.22) | 1,057.06 (-30.43) | 853.95 (-42.54) | 401.08 (-36.15) |
| R^2 | 0.96 | 0.83 | 0.83 | 0.96 | 0.97 | 0.84 | 0.92 | 0.96 | 0.96 | 0.96 | 0.97 | 0.99 | 0.97 | 0.93 |
| Adj. R^2 | 0.96 | 0.82 | 0.82 | 0.96 | 0.97 | 0.83 | 0.92 | 0.96 | 0.95 | 0.96 | 0.97 | 0.99 | 0.97 | 0.93 |

Table 4. Contemporaneous and 30-Day Lagged Spillovers

This table presents the estimated residuals that indicate the contagion effects between markets. The residuals are estimated from the following VAR model: $x_t = \Phi_1 x_{t-1} + \Phi_2 x_{t-2} + \dots + \Phi_p x_{t-p} + \varepsilon_t$. Panels (a) and (b) show contemporaneous and 30-day lagged spillover effects, respectively. * indicates statistical significance at the 10% level.

Panel (a): Contemporaneous Spillovers

| | Asia-Pacific | | | | | | | | Europe | | | | | | | | | | | America | | | | | | |
|--------------|--------------|------|------|------|------|------|-------|------|-----------|-------|-------|-----------|-------|------|-------|-------|------|-------|-----------|-----------|-------|------|-----------|-------|----|---|
| | AU | JP | KR | TW | CN | HK | TH | IN | <u>CH</u> | GR | TR | <u>IL</u> | DE | AT | DK | SE | NO | UK | <u>NL</u> | <u>IT</u> | FR | RU | <u>US</u> | CA | BR | |
| Asia-Pacific | AU | 100* | 0 | 0 | 0 | 0 | 0 | 0 | 0 | 0 | 0 | 0 | 0 | 0 | 0 | 0 | 0 | 0 | 0 | 0 | 0 | 0 | 0 | 0 | 0 | 0 |
| | JP | 0 | 100* | 0 | 0 | 0 | 0 | 0 | 0 | 0 | 0 | 0 | 0 | 0 | 0 | 0 | 0 | 0 | 0 | 0 | 0 | 0 | 0 | 0 | 0 | 0 |
| | KR | 0 | 0 | 100* | 0 | 0 | 0 | 0 | 0 | 0 | 0 | 0 | 0 | 0 | 0 | 0 | 0 | 0 | 0 | 0 | 0 | 0 | 0 | 0 | 0 | 0 |
| | TW | 0 | 0 | 0 | 100* | 0 | 0 | 0 | 0 | 0 | 0 | 0 | 0 | 0 | 0 | 0 | 0 | 0 | 0 | 0 | 0 | 0 | 0 | 0 | 0 | 0 |
| | CN | 0 | 0 | 0 | 0 | 100* | 0 | 0 | 0 | 0 | 0 | 0 | 0 | 0 | 0 | 0 | 0 | 0 | 0 | 0 | 0 | 0 | 0 | 0 | 0 | 0 |
| | <u>HK</u> | 0 | 0 | 0 | 0 | 0 | 80.3* | 9 | 3 | 0 | 0 | 0 | 7.9* | 0 | 0 | 0 | 0 | 0 | 0 | 0 | 0 | 0 | 0 | 0 | 0 | 0 |
| | TH | 0 | 0 | 0 | 0 | 0 | 0 | 100* | 0 | 0 | 0 | 0 | 0 | 0 | 0 | 0 | 0 | 0 | 0 | 0 | 0 | 0 | 0 | 0 | 0 | 0 |
| | <u>IN</u> | 0 | 0 | 0 | 0 | 0 | 0 | 0 | 64.1* | 0 | 0 | 0 | 35.9* | 0 | 0 | 0 | 0 | 0 | 0 | 0 | 0 | 0 | 0 | 0 | 0 | 0 |
| Europe | <u>CH</u> | 0 | 0 | 0 | 0 | 0 | 0 | 0 | 91.8* | 0 | 0 | 0 | 0 | 0 | 0 | 0 | 0 | 0 | 0 | 0 | 0 | 0 | 8.2* | 0 | 0 | |
| | <u>GR</u> | 0 | 0 | 0 | 0 | 0 | 0 | 0 | 13.0* | 70.9* | 0 | 0 | 0 | 0 | 0 | 0 | 0 | 4 | 0 | 0 | 0 | 2 | 10.0* | 0 | 0 | |
| | TR | 0 | 0 | 0 | 0 | 0 | 0 | 0 | 0 | 0 | 97.6* | 0 | 0 | 0 | 0 | 0 | 2 | 0 | 0 | 0 | 0 | 0 | 0 | 0 | 0 | |
| | IL | 0 | 0 | 0 | 0 | 4 | 0 | 0 | 0 | 0 | 0 | 96.5* | 0 | 0 | 0 | 0 | 0 | 0 | 0 | 0 | 0 | 0 | 0 | 0 | 0 | |
| | <u>DE</u> | 0 | 0 | 0 | 0 | 0 | 0 | 0 | 0 | 0 | 0 | 0 | 50.3* | 0 | 0 | 0 | 0 | 0 | 49.7* | 0 | 0 | 0 | 0 | 0 | 0 | |
| | AT | 0 | 0 | 0 | 0 | 0 | 0 | 0 | 0 | 0 | 0 | 0 | 0 | 100* | 0 | 0 | 0 | 0 | 0 | 0 | 0 | 0 | 0 | 0 | 0 | |
| | <u>DK</u> | 0 | 0 | 0 | 0 | 0 | 0 | 0 | 34.8* | 0 | 0 | 0 | 0 | 0 | 48.9* | 0 | 0 | 0 | 0 | 13.9* | 2 | 0 | 0 | 0 | 0 | |
| | <u>SE</u> | 0 | 0 | 0 | 0 | 0 | 0 | 0 | 16.9* | 0 | 0 | 0 | 0 | 0 | 0 | 65.9* | 1 | 0 | 0 | 0 | 0 | 0 | 16.0* | 0 | 0 | |
| | NO | 0 | 0 | 0 | 0 | 0 | 0 | 0 | 0 | 0 | 0 | 0 | 0 | 0 | 0 | 0 | 100* | 0 | 0 | 0 | 0 | 0 | 0 | 0 | 0 | |
| | <u>UK</u> | 0 | 0 | 0 | 1 | 0 | 0 | 0 | 15.2* | 0 | 0 | 0 | 1 | 0 | 0 | 5 | 0 | 58.9* | 0 | 1 | 0 | 0 | 17.0* | 0 | 0 | |
| | NL | 0 | 0 | 0 | 0 | 0 | 0 | 0 | 0 | 0 | 0 | 0 | 0 | 4 | 0 | 0 | 0 | 0 | 95.7* | 0 | 0 | 0 | 0 | 0 | 1 | |
| | <u>IT</u> | 0 | 0 | 0 | 0 | 0 | 0 | 0 | 18.6* | 0 | 0 | 0 | 0 | 2 | 0 | 4 | 0 | 0 | 0 | 76.2* | 0 | 0 | 0 | 0 | 0 | |
| | <u>FR</u> | 0 | 0 | 0 | 0 | 0 | 0 | 0 | 0 | 0 | 0 | 0 | 0 | 0 | 0 | 12.9* | 0 | 0 | 0 | 14.5* | 71.2* | 1 | 0 | 0 | 0 | |
| | RU | 0 | 0 | 0 | 0 | 0 | 0 | 0 | 0 | 0 | 0 | 0 | 0 | 0 | 0 | 0 | 0 | 0 | 0 | 0 | 0 | 100* | 0 | 0 | 0 | |
| America | US | 0 | 0 | 0 | 0 | 0 | 0 | 0 | 0 | 0 | 0 | 0 | 0 | 0 | 0 | 0 | 0 | 0 | 0 | 0 | 0 | 0 | 100* | 0 | 0 | |
| | CA | 0 | 0 | 0 | 2 | 0 | 0 | 0 | 0 | 0 | 0 | 0 | 0 | 0 | 0 | 0 | 0 | 0 | 0 | 0 | 0 | 0 | 2 | 95.5* | 0 | |

Table 5. Determinants of the Directed Spillover Effects

This table reports the estimation results for the determinants of the directed spillover effects. The columns labeled *OLS* show the estimation results for ordinary least squares regressions. The column labeled *FE* shows the results of estimating fixed-effect panel data regressions. Finally, the column labeled *FE+Year* shows the results of estimating panel data regressions controlling for fixed individual market and year effects. *Return*, *Trend*, *Volatility*, *ATM*, *TermSpread*, *MOVE*, *VIX*, *Crisis*, and *Euro Debt* denote the spot market return, the spot market trend, the spot market volatility, the term spread in the bond market, the MOVE index for the bond market, the VIX index for the options market, a dummy variable for the global financial crisis, and a dummy variable for the European debt crisis, respectively. *Constant* is a constant term. The row labeled *Individual Effect* indicates whether the given model includes individual market fixed effects, and the row labeled *Time Effect* indicates whether the given model includes year effects. *N* is the number of observations. R^2 (*Adj. R²*) is the *R*-squared (adjusted *R*-squared) value. *F*-statistics denotes the results of the *F*-test for model fitness. Numbers in parentheses are *t*-statistics. ** and *** indicate significance at the 5% and 1% levels, respectively.

| | (1) | (2) | (3) | (4) | (5) |
|---------------------------|----------------------|-----------------------|-----------------------|----------------------|----------------------|
| | OLS | OLS | OLS | FE | FE+Year |
| Return | -2.21 (-1.18) | -0.20 (-0.11) | -0.87 (-0.46) | -1.31 (-0.92) | -1.53 (-1.08) |
| Trend | -2.15*** (-12.76) | -1.25*** (-7.11) | -1.41*** (-7.90) | -0.72*** (-5.27) | -0.67*** (-4.58) |
| Volatility | -22.31*** (-6.97) | -50.29*** (-13.90) | -40.05*** (-10.82) | 0.89 (-0.31) | 3.82 (-1.23) |
| ATM | -0.03*** (-22.01) | -0.04*** (-26.22) | -0.04*** (-26.19) | -0.01*** (-8.93) | -0.01*** (-8.27) |
| TermSpread | -0.02*** (-7.12) | 0.00 (-0.29) | -0.01*** (-3.02) | -0.02*** (-13.64) | -0.02*** (-13.42) |
| MOVE | | -0.00*** (-4.75) | 0.00 (-0.98) | 0.00** (-2.45) | 0.00 (-0.42) |
| VIX | | 0.04*** (-16.62) | 0.03*** (-11.86) | 0.00 (-0.89) | -0.01** (-2.45) |
| Crisis | | | -0.17*** (-3.15) | -0.09** (-2.23) | -0.14** (-2.34) |
| Euro Debt | | | 0.32*** (-12.39) | 0.29*** (-14.71) | 0.24*** (-3.14) |
| Constant | 4.52*** (177.71) | 4.19*** (103.98) | 3.91*** (83.47) | 2.41*** (49.36) | 2.15*** (24.87) |
| Individual Effect | NO | NO | NO | YES | YES |
| Time Effect | NO | NO | NO | NO | YES |
| N | 43,184 | 43,184 | 43,184 | 43,184 | 4,318 |
| R² | 0.04 | 0.05 | 0.05 | 0.46 | 0.46 |
| Adj. R² | 0.04 | 0.05 | 0.05 | 0.46 | 0.46 |
| F-statistics | 353.15 | 301.71 | 256.50 | 1,505.23 | 1,041.16 |

